Laser and Particle Beams (2012), *30*, 291–298.

doi:10.1017/S0263034612000092

Second and third harmonics generation in the interaction of strongly magnetized dense plasma with an intense laser beam

MOHAMMAD GHORBANALILU

Physics Department, Azarbaijan University of Tarbiat Moallem, Tabriz, Iran; Plasma & Condensed Matter Computational Research Lab, Azarabaijan University of Tabiat Moallem, Tabriz, Iran

(Received 29 September 2011; Accepted 13 February 2012)

Abstract

The goal of this theory is to study the conversion of a fraction of a laser beam to its phase-mismatch second and third harmonics. This conversion takes place by focusing an intense laser beam into a transversely magnetized plasma, as a nonlinear medium. The influence of the polarization field is considered, however, the plasma density is below the critical density. It has already been revealed that for dense plasma, the second and third harmonics efficiencies decreased with density increasing in the presence of a sufficiently strong magnetic field. This result is in contrast to the under dense and weakly magnetized plasma, which the harmonics efficiencies increased with density increasing. It is shown that the harmonics radiation cut-off, when the magnetic field increases up until the saturation strength Bsat. In addition, the results indicated that the average phase-mismatch third harmonic conversion efficiency is a little smaller than the phase-match case reported for non-magnetized plasma.

Keywords: Harmonic generation; Laser plasma interaction; Magnetized plasma

1. INTRODUCTION

Study of intense laser propagating through plasma is of interest for wide range of applications, such as laser wakefield acceleration (Tajima & Dawson, 1979; Jha *et al.*, 2005), plasma based light source (Mori, 1993), X-ray laser (Amendt *et al.*, 1991; Lemoff *et al.*, 1995), optical harmonic generation (Sprangle *et al.*, 1990; Lin *et al.*, 2002), inertial confinement fusion (Tabak *et al.*, 1994), and so on. These applications provide strong motivation to encourage the studying of laser-plasma interaction, so this area has always been a fundamental topic in theoretical plasma physics in the past decades. On the other hand, owing to the generation of a hundred megaguass quasi-static magnetic field in laser plasma interaction (Gorbunov *et al.*, 1997), the analysis of laser interaction with magnetized plasma was always an important issue for a real plasma system.

The harmonic generation is a nonlinear phenomenon in which the electrons oscillating in high-intensity laser fields is surveyed and assessed as a means of producing short-wavelength radiation sources. This phenomenon engaged scientists to clarify the mechanisms and methods of high-order harmonic generation.

Recently, high-order nonlinear effects have attracted great attention with the development of ultrafast laser technology. When we focus on an intense laser pulse into a gas, strong nonlinear interactions can lead to the generation of very high odd harmonics of the optical frequency of the pulse (Corkum, 1993; Salieres & Lewenstein, 2001). This effect typically occurs at optical intensities on the order of $10^{14}\ \mathrm{W/cm^2}$ or higher. Although only a tiny fraction of the laser power can be converted into higher harmonics, this output can still be useful for technical applications (Kienberger, 2004).

The previous reports indicated that only the odd harmonics can be generated in the laser interaction with homogenous plasma (Esarey *et al.*, 1993; Gibbon, 1997; Mori *et al.*, 1993; Wilks *et al.*, 1993), however, in the presence of a modulated transverse magnetic field, the phase-match second harmonic generation has been investigated (Rax & Fisch, 1992). Beside, the phase-mismatch second harmonic generation has been reported for the laser field interaction with underdense transversely magnetized plasma (jha *et al.*, 2007).

When a strong magnetic field applied into a plasma, the electron dynamic modified, and this leads to the nonlinear current modification. Therefore, it is reasonable that the

Address correspondence and reprint requests to: Mohammad Ghorbanalilu, Physics Department, Azarbaijan University of Tarbiat Moallem, Tabriz, Iran. E-mail: mh-alilo@yahoo.com

magnetic field makes affect the harmonics generation. When the density perturbation produced by magnetic field coupled with electron quiver motions, it is plausible to generate the second harmonic (jha *et al.*, 2007).

In this paper, we investigate the phase-mismatch second and third harmonics generation in the interaction of intense laser beam and transversely magnetized plasma, when the plasma is dense and applied, magnetic field is strong. This report may be applicable in the wide range of external magnetic field strength and plasma density, in contrast to the pervious report for second harmonic generation that has been performed for underdense weakly magnetized plasma in the absence of the polarization field (jha *et al.*, 2007).

This paper is organized in four section. In Section 2, by using the perturbative technique in mildly relativistic and weakly nonlinear regime ($a_1 < 1$), induced nonlinear current density due to the interaction of intense laser beam with transversely magnetized plasma is derived for the second and third harmonics. In Section 3, the nonlinear wave equation solved for vector potential of driving laser beam, and the conversion efficiencies are obtained for the phase-mismatch second and third harmonics. Finally, a summary and conclusion is presented in Section 4.

2. NON-LINEAR CURRENT DENSITY

We assume the linearly polarized vector potential for nth harmonic is given as:

$$\vec{A}_n = \vec{e}_x A_n(z, r, t)\sin(k_n z - n\omega_0 t). \tag{1}$$

Here, A_n, $n\omega_0$ and $k_n = (n\omega_0/c)\epsilon_n^{1/2}$ are the amplitude, frequency, and wavevector of the nth harmonic, in which the ϵ_n introduces the dielectric permittivity at frequency $n\omega_0$. The fundamental harmonic characteristics yield with $n = 1$.

We know the motion of charge particles in the presence of the intense laser beam and external magnetic field are described by relativistic Lorentz equation as:

$$\frac{d(\gamma\vec{v})}{dt} = -\frac{e}{m}\left[\vec{E}_1 + \vec{E} + \vec{v}\times(\vec{B}_0 + \vec{B})\right]. \tag{2}$$

Here E_1 is the laser field amplitude, $\vec{B} = (\vec{k_1}\times\vec{E_1})/\omega_0$ and $\vec{B_0} = \vec{e}_y B_0$ are the magnetic field of propagating laser beam and external magnetic field, respectively. Additionally, $\vec{E}$ is the polarization field due to the charge separation, and $\gamma = (1 + p^2/m^2c^2)^{1/2}$ is the relativistic factor. The ponderomotive force $-e(\vec{v}\times\vec{B})$ pushes the electrons in the direction of the laser beam propagation and the polarization field E_z generated owing to the charge separation in the z direction. Furthermore, the force $-e(\vec{v}\times\vec{B_0})$, which arises to the external magnetic field has a component in the z direction, and so the strong magnetic field can be affect the charge separation efficiently. However, the ponderomotive force is smaller in plan wave with respect to the Gaussian profile short pulse beam, but for strongly magnetized plasma the influence of the z component of the force $-e(\vec{v}\times\vec{B_0})$ is very dominate for the charge separation process and the polarization field generation.

Using the perturbative theory in Eq. (2), and continuity equation $(\partial n/\partial t + \vec{\nabla}.(n\vec{v}) = 0)$, it is possible to expand all quantities in terms of the order of the radiation field. In this method, the relativistic effect comes into play in the third order velocity components and higher. If we consider the plasma is cold and the electrons are at rest before the laser field is applied, the first order equations for the electron velocity components, in accord to this technique, is written as:

$$\begin{aligned}\frac{\partial v_x^{(1)}}{\partial t} &= -\frac{eE_1}{m} + \omega_c v_z^{(1)},\\ \frac{\partial v_z^{(1)}}{\partial t} &= -\frac{eE_z^{(1)}}{m} - \omega_c v_x^{(1)},\\ \frac{\partial v_y^{(1)}}{\partial t} &= 0,\end{aligned} \tag{3}$$

where $E_z^{(1)}$, $E_1 = -\partial A_1/\partial t$, $\omega_c = eB_0/m$, are the first order perturbation for polarization field, laser field amplitude, and the electron cyclotron frequency, respectively. By taking a time derivative of the second relation in Eq. (3), also using the first relation, and estimate the relative term to the first order of the polarization field $(\partial E_z^{(1)}/\partial z = -e\,n^{(1)}/\epsilon_0)$ as below:

$$\begin{aligned}-\frac{e}{m}\frac{\partial}{\partial t}E_z^{(1)} &= \frac{e^2}{m\epsilon_0}\int\frac{\partial}{\partial t}n^{(1)}dz\\ &= -\frac{e^2}{m\epsilon_0}\int\left[\frac{\partial}{\partial z}(n_0 v_z^{(1)})\right]dz = -\omega_p^2 v_z^{(1)},\end{aligned} \tag{4}$$

we arrive

$$\frac{\partial^2 v_z^{(1)}}{\partial t^2} + \omega_p^2 v_z^{(1)} + \omega_c^2 v_z^{(1)} = a_1 c\omega_0\omega_c\cos\varphi, \tag{5}$$

where $a_1 = eE_1/mc\omega_0$, $\omega_p = (ne^2/m\epsilon_0)^{1/2}$, and n_0 are the normalized laser field amplitude (or normalized vector potential $a_1 = eA_1/mc$), plasma frequency, and unperturbed electron density, respectively, also $\varphi = k_1 z - \omega_0 t$. Eq. (4) indicates that the polarization field oscillates as the same frequency with $v_z^{(1)}$, or the laser field frequency. This means that the polarization field is not slow and it is reasonable that this field makes affect the harmonic generation. The solution of Eq. (5) and performing the same steps for component v_x, the first order electron velocity components are given by:

$$\begin{aligned}v_x^{(1)} &= \frac{a_1 c(\omega_0^2 - \omega_p^2)}{(\omega_0^2 - \omega_p^2 - \omega_c^2)}\sin\varphi\\ v_z^{(1)} &= -\frac{a_1 c\omega_c\omega_0}{(\omega_0^2 - \omega_p^2 - \omega_c^2)}\cos\varphi.\end{aligned} \tag{6}$$

By following the same steps for the nth harmonic, the first order velocity components yield only by substituting ω_0

$\rightarrow n\omega_0$, $a_1 \rightarrow a_n$ and $\varphi \rightarrow k_n z - n\omega_0 t$, into Eq. (6). Therefore, the linear part of the induced current density corresponding to the nth harmonic, $J_x^{(1)}(n\omega_0) = -n_0 e\, v_x^{(1)}(n\omega_0)$, can be written as:

$$J_x^{(1)}(n\omega_0) = -\frac{n_0 e a_n c(\omega_0^2 - \omega_p^2)}{(n^2\omega_0^2 - \omega_p^2 - \omega_c^2)} \sin(k_n z - n\omega_0 t), \tag{7}$$

where $a_n = eA_n/mc$ is the normalized vector potential for nth harmonic. Substituting Eq. (7) into the wave equation for nth harmonic, it is possible to derive the linear dispersion equation as:

$$c^2 k_n^2 = n^2\omega_0^2 - \frac{\omega_p^2(n^2\omega_0^2 - \omega_p^2)}{(n^2\omega_0^2 - \omega_p^2 - \omega_c^2)}. \tag{8}$$

Using Eq. (8) into the well known transverse wave dispersion equation $k_n = (n\omega_0/c)\epsilon_n^{1/2}$, the plasma permittivity corresponding to the frequency $n\omega_0$ is given by:

$$\epsilon_n = 1 - \frac{\omega_p^2(n^2\omega_0^2 - \omega_p^2)}{n^2\omega_0^2(n^2\omega_0^2 - \omega_p^2 - \omega_c^2)}. \tag{9}$$

It is important to note that, the effect of polarization field is included in deriving the Eq. (9).

It is intuitively understood that electron density is disturbed when a driving laser beam propagate through the plasma. The spatiotemporal variations for electron perturbations are given by the continuity equation. Therefore, similarly to the velocity components, we can expand the electron density in terms on the order of the radiation field. Then in accordance to the continuity equation and Eq. (6), the first order electron density perturbation takes the form as:

$$n^{(1)} = -\int \frac{\partial}{\partial z}(n_0 v_z^{(1)})dt = -\frac{a_1 n_0 c k_1 \omega_c}{(\omega_0^2 - \omega_p^2 - \omega_c^2)} \cos\varphi. \tag{10}$$

Now, we are on the stage to obtain the second order velocity components. In doing so, similar to the first order, by the same procedure the coupled equations arise from the relativistic Lorentz equation are given by:

$$\begin{aligned} &\frac{\partial v_x^{(2)}}{\partial t} + v_z^{(1)}\frac{\partial v_x^{(1)}}{\partial z} = \omega_c v_z^{(2)} + \frac{eB}{m} v_z^{(1)} \\ &\frac{\partial v_z^{(2)}}{\partial t} + v_z^{(1)}\frac{\partial v_z^{(1)}}{\partial z} = -\frac{e}{m}E_z^{(2)} - \omega_c v_x^{(2)} - \frac{eB}{m} v_x^{(1)}, \end{aligned} \tag{11}$$

where $E_z^{(2)}$ is the second order perturbation for polarization field. After some mathematical processes, we arrive to the following partial differential equation for the z component of the second order of the electron velocity as:

$$\begin{aligned} \frac{\partial^2 v_z^{(2)}}{\partial t^2} + \omega_p^2 v_z^{(2)} + \omega_c^2 v_z^{(2)} = &-\frac{a_1^2 c^2 k_1 \omega_0 \omega_c^2(\omega_p^2 + \omega_c^2)}{2(\omega_0^2 - \omega_p^2 - \omega_c^2)^2} \\ &+ \frac{a_1^2 c^2 k_1 \omega_c\left[2(\omega_0^2 - \omega_p^2)^2 - \omega_c^2(4\omega_0^2 - \omega_p^2 + \omega_c^2)\right]}{2(\omega_0^2 - \omega_p^2 - \omega_c^2)^2} \cos 2\varphi. \end{aligned} \tag{12}$$

The solution of Eq. (12) give us the component $v_z^{(2)}$, so by the same procedure it is possible to find the component $v_x^{(2)}$. Therefore, the second order velocity components, easily, find as:

$$\begin{aligned} v_x^{(2)} &= \frac{a_1^2 c^2 k_1 \omega_c\left[(\omega_0^2 - \omega_p^2)^2 - \omega_c^2(4\omega_0^2 - \omega_p^2)\right]}{2(\omega_0^2 - \omega_p^2 - \omega_c^2)^2(4\omega_0^2 - \omega_p^2 - \omega_c^2)} \sin 2\varphi \\ v_z^{(2)} &= -\frac{a_1^2 c^2 k_1 \omega_c^2 \omega_0(\omega_p^2 + \omega_c^2)}{2(\omega_0^2 - \omega_p^2 - \omega_c^2)^2} \\ &\quad - \frac{a_1^2 c^2 k_1 \omega_0\left[2(\omega_0^2 - \omega_p^2)^2 - \omega_c^2(4\omega_0^2 - \omega_p^2 + \omega_c^2)\right]}{2(\omega_0^2 - \omega_p^2 - \omega_c^2)^2(4\omega_0^2 - \omega_p^2 - \omega_c^2)} \cos 2\varphi. \end{aligned} \tag{13}$$

It is clear from Eq. (13), the second order velocity components oscillate with frequency twice the laser field frequency. This effect arises from the external magnetic field, and coupling between the external and propagating magnetic fields.

The second order electron density perturbation is derived by the same method presented for $n^{(1)}$ as:

$$n^{(2)} = -\frac{a_1^2 n_0 c^2 k_1^2[(\omega_0^2 - \omega_p^2)^2 - \omega_c^2(4\omega_0^2 - \omega_p^2)]}{(\omega_0^2 - \omega_p^2 - \omega_c^2)^2(4\omega_0^2 - \omega_p^2 - \omega_c^2)} \cos 2\varphi. \tag{14}$$

Finally, we can expand the Lorentz equation in terms of the third order of the radiation field. Note that in this case, the relativistic factor play an important role in electron dynamic. The coupled equations for velocity components written as:

$$\begin{aligned} &\frac{\partial v_x^{(3)}}{\partial t} + \frac{\partial(\gamma^{(2)} v_x^{(1)})}{\partial t} + v_z^{(1)}\frac{\partial v_x^{(2)}}{\partial z} + v_z^{(2)}\frac{\partial v_x^{(1)}}{\partial z} \\ &\quad = \omega_c v_z^{(3)} + \frac{eB}{m} v_z^{(2)} \\ &\frac{\partial v_z^{(3)}}{\partial t} + \frac{\partial(\gamma^{(2)} v_z^{(1)})}{\partial t} + v_z^{(1)}\frac{\partial v_z^{(2)}}{\partial z} + v_z^{(2)}\frac{\partial v_z^{(1)}}{\partial z} \\ &\quad = -\frac{eE_z^{(3)}}{m} - \omega_c v_x^{(3)} - \frac{eB}{m} v_x^{(2)}, \end{aligned} \tag{15}$$

where $E_z^{(3)}$ and $\gamma^{(2)} = [(v_x^{(1)})^2 + (v_z^{(1)})^2]/2c^2$ are the third order perturbation for polarization field and the relativistic factor. By using some careful mathematical processes, similar to the first and second orders, we will get to the following

https://doi.org/10.1017/S0263034612000092 Published online by Cambridge University Press

results for the third order velocity components as:

$$v_x^{(3)} = -\frac{a_1^3 c}{8(\omega_0^2-\omega_p^2-\omega_c^2)^3}\left[\frac{A_\varphi+\omega_c^2 B_\varphi}{(\omega_0^2-\omega_p^2-\omega_c^2)}\sin\varphi + \frac{A_3\varphi+\omega_c^2 B_3\varphi}{(9\omega_0^2-\omega_p^2-\omega_c^2)}\sin 3\varphi\right]$$
$$v_z^{(3)} = \frac{a_1^3 c}{8(\omega_0^2-\omega_p^2-\omega_c^2)^3}\left[\frac{C_\varphi+D_\varphi}{(\omega_0^2-\omega_p^2-\omega_c^2)}\cos\varphi + \frac{C_3\varphi+D_3\varphi}{(9\omega_0^2-\omega_p^2-\omega_c^2)}\cos 3\varphi\right], \tag{16}$$

where,

$$A_\varphi = (3\omega_0^8 - 12\omega_0^6\omega_p^2 + 2\omega_0^6\omega_c^2 + 18\omega_0^4\omega_p^4 + 3\omega_0^4\omega_c^4 - 12\omega_0^2\omega_p^6 - 4\omega_0^4\omega_p^2\omega_c^2 + 2\omega_0^2\omega_p^4\omega_c^2 + 3\omega_p^8),\ B_\varphi = \frac{c^2k_1^2}{4\omega_0^2-\omega_p^2-\omega_c^2}(10\omega_0^6 - 18\omega_0^4\omega_p^2 + 10\omega_0^4\omega_c^2 + 6\omega_0^2\omega_p^4 - 20\omega_0^2\omega_c^4 - 14\omega_0^2\omega_p^2\omega_c^2 + 2\omega_p^6 + 4\omega_p^4\omega_c^2 + 2\omega_p^2\omega_c^4),$$
$$A_{3\varphi} = (-\,9\omega_0^8 + 28\omega_0^6\omega_p^2 + 6\omega_0^6\omega_c^2 - 30\omega_0^4\omega_p^4 + 3\omega_0^4\omega_c^4 + 12\omega_0^2\omega_p^6 - 4\omega_0^4\omega_p^2\omega_c^2 - 2\omega_0^2\omega_p^4\omega_c^2 + \omega_p^8),$$
$$B_{3\varphi} = \frac{c^2k_1^2}{4\omega_0^2-\omega_p^2-\omega_c^2}(34\omega_0^6 - 66\omega_0^4\omega_p^2 - 86\omega_0^4\omega_c^2 + 30\omega_0^2\omega_p^4 - 20\omega_0^2\omega_c^4 + 10\omega_0^2\omega_p^2\omega_c^2 + 2\omega_p^6 + 4\omega_p^4\omega_c^2 + 2\omega_p^2\omega_c^4),\ C_\varphi = (4\omega_0^6 - 11\omega_0^4\omega_p^2 + 4\omega_0^4\omega_c^2 + 10\omega_0^2\omega_p^4 - \omega_0^2\omega_p^2\omega_c^2 - 3\omega_p^6),\ D_\varphi = \frac{c^2k_1^2}{4\omega_0^2-\omega_p^2-\omega_c^2}(2\omega_0^6 + 6\omega_0^4\omega_p^2,\ + 26\omega_0^4\omega_c^2 - 18\omega_0^2\omega_p^4 - 22\omega_0^2\omega_c^4 - 40\omega_0^2\omega_p^2\omega_c^2 + 10\omega_p^6 + 14\omega_p^4\omega_c^2 - 2\omega_p^2\omega_c^4 - 6\omega_c^4),\ C_{3\varphi} = (-\,12\omega_0^6 + 27\omega_0^4\omega_p^2 + 12\omega_0^4\omega_c^2 - 18\omega_0^2\omega_p^4 - 3\omega_0^2\omega_p^2\omega_c^2 + 3\omega_p^6),$$
$$D_{3\varphi} = \frac{c^2k_1^2}{4\omega_0^2-\omega_p^2-\omega_c^2}(30\omega_0^6 - 46\omega_0^4\omega_p^2 - 34\omega_0^4\omega_c^2 + 2\omega_0^2\omega_p^4 - 66\omega_0^2\omega_c^4 - 64\omega_0^2\omega_p^2\omega_c^2 + 14\omega_p^6 + 26\omega_p^4\omega_c^2 + 10\omega_p^2\omega_c^4 - 2\omega_c^6).$$

In view of the fact that the harmonics are driven by the nonlinear current, we can evaluate this source term using the perturbed quantities obtained previously. According to the current density carried by the electrons $J = -nev$, the second order nonlinear current density for the second harmonic, $J_x^{(2)} = -e(n_0 v_x^{(2)} + n^{(1)}\ v_x^{(1)})$, after substituting the required quantities, written as:

$$J_x^{(2)}(2\omega_0) = \frac{3a_1^2 n_0 e c^2 k_1 \omega_0^2 \omega_c(\omega_0^2-\omega_p^2+\omega_c^2)}{2(\omega_0^2-\omega_p^2-\omega_c^2)^2(4\omega_0^2-\omega_p^2-\omega_c^2)}\sin 2\varphi. \tag{17}$$

To proceed further, we find the third order current density for third harmonic, $J_x^{(3)} = -e(n_0\ v_x^{(3)} + n^{(1)}\ v_x^{(2)} + n^{(2)}\ v_x^{(1)})$ as:

$$J_x^{(3)}(3\omega_0) = \frac{a_1^3 n_0 e c}{8(\omega_0^2-\omega_p^2-\omega_c^2)^3(9\omega_0^2-\omega_p^2-\omega_c^2)} \times\left[\left(A'_{3\varphi} + \frac{c^2k_1^2}{(4\omega_0^2-\omega_p^2-\omega_c^2)}B'_{3\varphi}\right)\sin 3\varphi\right], \tag{18}$$

where,

$$A'_{3\varphi} = (-\,9\omega_0^8 + 28\omega_0^6\omega_p^2 + 6\omega_0^6\omega_c^2 - 30\omega_0^4\omega_p^4 + 3\omega_0^4\omega_c^4 + 12\omega_0^2\omega_p^6 - 4\omega_0^4\omega_p^2\omega_c^2 - 2\omega_0^2\omega_p^4\omega_c^2 - \omega_p^8),$$
$$B'_{3\varphi} = (36\omega_0^8 - 112\omega_0^6\omega_p^2 - 96\omega_0^6\omega_c^2 + 120\omega_0^4\omega_p^4 - 144\omega_0^4\omega_c^4 - 48\omega_0^2\omega_p^6 - 12\omega_0^2\omega_c^6 + 104\omega_0^4\omega_p^2\omega_c^2 - 16\omega_0^2\omega_p^4\omega_c^2 + 20\omega_0^2\omega_p^2\omega_c^4 + 4\omega_p^8 + 8\omega_p^6\omega_c^2 + 4\omega_p^4\omega_c^4).$$

3. CONVERSION EFFICIENCY

The above expressions for the harmonic components of the source current, $J_x^{(2)}(2\omega_0)$ and $J_x^{(3)}(3\omega_0)$, can be used in the following wave equation, to determine the growth of harmonics radiation.

$$\left(\frac{\partial^2}{\partial z^2} - \frac{1}{c^2}\frac{\partial^2}{\partial t^2} - \frac{\omega_p^2}{c^2}\right)a_n = -\frac{e}{\epsilon_0 m c^3}J_x^{(n)}(n\omega_0), \tag{19}$$

where subscript n refers to the order of harmonic. We obtained this source term in the previous section, thus the vector potential amplitude can be evaluate by solution the wave equation. The steady state amplitude for the phase-mismatch second harmonic obtained by suggestion $a_2 = a_2(z)e^{i(k_2 z - 2\omega_0 t)}/2 + c.c$ into Eq. (19), and making used of the Eq. (17).

Assuming that $\partial^2 a_2(z)/\partial z^2 \ll k_2\partial\ a_2(z)/\partial z$, which means that $\partial a_2(z)/\partial z$ changes appreciably larger than wavelength $2\pi/k_2$, and for $4\omega_0^2 \gg \omega_c^2$, we arrive the normalized amplitude for the phase-mismatch second harmonic as below:

$$a_2(z) = \frac{3a_1^2\omega_c}{16c}\frac{\omega_p^2}{\omega_0^2} \times \frac{\left[1-\frac{\omega_p^2}{\omega_0^2}\left(1-\frac{\omega_p^2}{\omega_0^2}\right)\left(1-\frac{\omega_c^2}{\omega_0^2}-\frac{\omega_p^2}{\omega_0^2}\right)^{-1}\right]^{1/2}}{\left[1-\frac{\omega_p^2}{4\omega_0^2}\left(1-\frac{\omega_p^2}{4\omega_0^2}\right)\left(1-\frac{\omega_c^2}{4\omega_0^2}-\frac{\omega_p^2}{4\omega_0^2}\right)^{-1}\right]^{1/2}} \times \frac{\left(1-\frac{\omega_p^2}{\omega_0^2}+\frac{\omega_c^2}{\omega_0^2}\right)}{\left(1-\frac{\omega_p^2}{\omega_0^2}-\frac{\omega_c^2}{\omega_0^2}\right)^2\left(1-\frac{\omega_p^2}{4\omega_0^2}-\frac{\omega_c^2}{4\omega_0^2}\right)} \times e^{i(\Delta k z)/2}\left(\frac{\sin(\Delta k.z/2)}{\Delta k}\right), \tag{20}$$

https://doi.org/10.1017/S0263034612000092 Published online by Cambridge University Press

where $\Delta k = 2k_1 - k_2$ is the wavevector mismatch for the second harmonic. Definitely, anyone find from Eq. (20) that the second harmonic can be generate only in the magneto-active plasmas, which may be considered as an important advantage for such kind of plasmas.

The normalized amplitude for the phase-mismatch third harmonic is obtained by the same procedure, by substituting $a_3 = a_3(z)e^{i(k_3 z - 3\omega_0 t)}/2 + c.c$ into Eq. (19) and using the Eq. (18), for $9\omega_0^2 \gg \omega_c^2$. The result is given by:

$$a_3(z) = \frac{\omega_p^2 a_1^3}{24\omega_0 c}\left[1 - \frac{\omega_p^2}{9\omega_0^2}\left(1 - \frac{\omega_p^2}{9\omega_0^2}\right)\left(1 - \frac{\omega_c^2}{9\omega_0^2} - \frac{\omega_p^2}{9\omega_0^2}\right)^{-1}\right]^{-1/2} \times \left\{\frac{\dfrac{A'_{3\varphi}}{\omega_0^8} + \left[1 - \dfrac{\omega_p^2}{\omega_0^2}\left(1 - \dfrac{\omega_p^2}{\omega_0^2}\right)\left(1 - \dfrac{\omega_c^2}{\omega_0^2} - \dfrac{\omega_p^2}{\omega_0^2}\right)^{-1}\right]\left(4 - \dfrac{\omega_p^2}{\omega_0^2} - \dfrac{\omega_c^2}{\omega_0^2}\right)^{-1} \times \dfrac{B'_{3\varphi}}{\omega_0^8}}{\left(1 - \dfrac{\omega_p^2}{\omega_0^2} - \dfrac{\omega_c^2}{\omega_0^2}\right)^3\left(9 - \dfrac{\omega_p^2}{\omega_0^2} - \dfrac{\omega_c^2}{\omega_0^2}\right)}\right\} \times e^{i(\Delta k' z)/2}\left(\frac{\sin(\Delta k'.z/2)}{\Delta k'}\right), \tag{21}$$

where $\Delta k' = 3k_1 - k_3$ is the wavevector mismatch for the third harmonic. Taking into account that the conversion efficiency for nth harmonic is defined as:

$$\eta_n = \frac{\epsilon_n^{1/2}\left|\dfrac{\partial a_n}{\partial t}\right|^2}{\epsilon_1^{1/2}\left|\dfrac{\partial a_1}{\partial t}\right|^2}, \tag{22}$$

we get the conversion efficiencies for the phase-mismatch second and third harmonics as below:

$$\eta_2(z) = \frac{9a_1^2\omega_c^2}{128c^2}\frac{\omega_p^4}{\omega_0^4}\frac{\left[1 - \dfrac{\omega_p^2}{\omega_0^2}\left(1 - \dfrac{\omega_p^2}{\omega_0^2}\right)\left(1 - \dfrac{\omega_c^2}{\omega_0^2} - \dfrac{\omega_p^2}{\omega_0^2}\right)^{-1}\right]^{1/2}}{\left[1 - \dfrac{\omega_p^2}{4\omega_0^2}\left(1 - \dfrac{\omega_p^2}{4\omega_0^2}\right)\left(1 - \dfrac{\omega_c^2}{4\omega_0^2} - \dfrac{\omega_p^2}{4\omega_0^2}\right)^{-1}\right]^{1/2}} \times \frac{\left(1 - \dfrac{\omega_p^2}{\omega_0^2} + \dfrac{\omega_c^2}{\omega_0^2}\right)^2}{\left(1 - \dfrac{\omega_p^2}{\omega_0^2} - \dfrac{\omega_c^2}{\omega_0^2}\right)^4\left(1 - \dfrac{\omega_p^2}{4\omega_0^2} - \dfrac{\omega_c^2}{4\omega_0^2}\right)^2} \times \left(\frac{\sin^2(\Delta k.z/2)}{(\Delta k)^2}\right). \tag{23}$$

$$\eta_3(z) = \frac{\omega_p^4 a_0^4}{192\omega_0^2 c^2}\frac{\left[1 - \dfrac{\omega_p^2}{\omega_0^2}\left(1 - \dfrac{\omega_p^2}{\omega_0^2}\right)\left(1 - \dfrac{\omega_c^2}{\omega_0^2} - \dfrac{\omega_p^2}{\omega_0^2}\right)^{-1}\right]^{-1/2}}{\left[1 - \dfrac{\omega_p^2}{9\omega_0^2}\left(1 - \dfrac{\omega_p^2}{9\omega_0^2}\right)\left(1 - \dfrac{\omega_c^2}{9\omega_0^2} - \dfrac{\omega_p^2}{9\omega_0^2}\right)^{-1}\right]^{1/2}} \times \frac{\left\{\dfrac{A'_{3\varphi}}{\omega_0^8} + \left[1 - \dfrac{\omega_p^2}{\omega_0^2}\left(1 - \dfrac{\omega_p^2}{\omega_0^2}\right)\left(1 - \dfrac{\omega_c^2}{\omega_0^2} - \dfrac{\omega_p^2}{\omega_0^2}\right)^{-1}\right]\left(4 - \dfrac{\omega_p^2}{\omega_0^2} - \dfrac{\omega_c^2}{\omega_0^2}\right)^{-1} \times \dfrac{B'_{3\varphi}}{\omega_0^8}\right\}^2}{\left(1 - \dfrac{\omega_p^2}{\omega_0^2} - \dfrac{\omega_c^2}{\omega_0^2}\right)^6\left(9 - \dfrac{\omega_p^2}{\omega_0^2} - \dfrac{\omega_c^2}{\omega_0^2}\right)^2} \times \left(\frac{\sin^2(\Delta k'.z/2)}{(\Delta k')^2}\right). \tag{24}$$

With a short look at Eqs. (23) and (24), it is found that the harmonics oscillate in magnitude around an average value due to the dephasing between the pump laser and the radiation harmonics. The maximum conversion efficiencies take place in the coherence lengths $z_c = \pi/\Delta k$ and $z'_c = \pi/\Delta k'$, respectively, for the second and third harmonics. Therefore, the power efficiencies are harmonic by z, so we have the points with maximum and minimum electric field amplitude for the radiation harmonics inside the plasma.

According to this fact that we deal with the strongly magnetized dense plasma, there is worry about that the laser beam may be damped or absorbed. The absorbtion occurs for $\epsilon_1 \rightarrow \infty$ and or $\omega_0^2 = \omega_p^2 + \omega_c^2$, however, any damping takes place for $\epsilon_1 < 0$.

In Figure 1, we show the damping and absorbing regions on the $(\omega_p/\omega_0 - \omega_c/\omega_0)$ plan. The hachured area predicts the damping region for the laser beam, while all points on the solid line satisfy the absorbtion condition. If the parameters ω_p/ω_0 and ω_c/ω_0 choose in such a manner that the corresponding point on the $(\omega_p/\omega_0 - \omega_c/\omega_0)$ plan is placed on the region $\epsilon_1 > 0$, the laser beam does not damp or absorb during propagating through the plasma.

The conversion efficiency $\%\eta_2$ for the second harmonic is plotted as a function of z/λ for $\omega_p/\omega_0 = 0.3$, and for different values of the external magnetic field, in Figure 2. We assume the pump laser is a Nd:Yag laser with intensity around 10^{17} W/cm^2 $(a_1 = 0.271)$ and frequency $\omega_0 = 1.88 \times 10^{15} s^{-1}$ and or wavelength $\lambda = 1$ μm. The figure shows the second harmonic efficiency reaches to the maximum value after that the laser beam traveling as coherence lengths 7.1 μm and 6.8 μm inside the plasma, respectively, for $\omega_c/\omega_0 = 0.1$ and $\omega_c/\omega_0 = 0.2$. Therefore, the coherence

https://doi.org/10.1017/S0263034612000092 Published online by Cambridge University Press

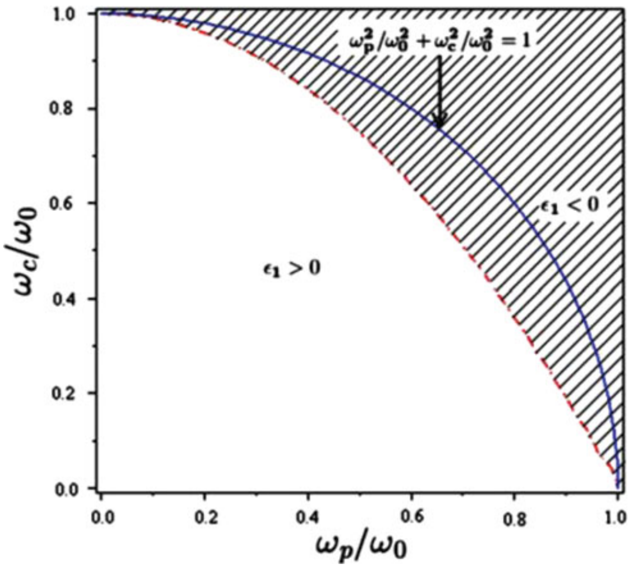

Fig. 1. (Color online) Schematic investigation for damping and absorbing region on the ($\omega_p/\omega_0 - \omega_c/\omega_0$) plan for the laser beam propagating through the plasma.

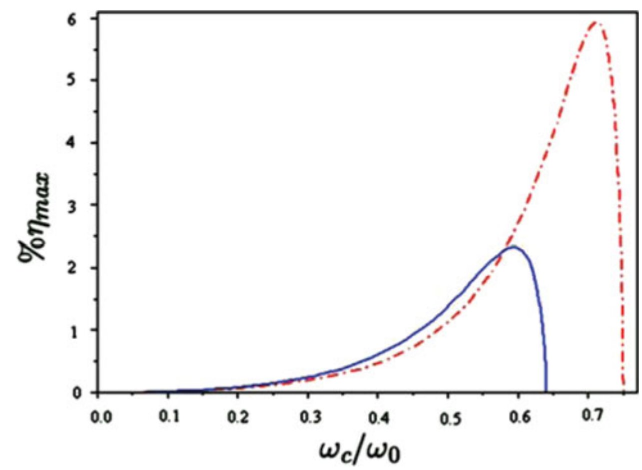

Fig. 3. (Color online) The maximum conversion efficiency variation for the phase-mismatch second harmonic with respect to the ω_c/ω_0, for $a_1 = 0.271$, respectively, the solid line for $\omega_p/\omega_0 = 0.6$, the dash dot line for $\omega_p/\omega_0 = 0.5$.

length for radiation harmonic decreases with magnetic field increasing. On the other hand, the figure demonstrates that the second harmonic conversion efficiency drastically increased with magnetic field increasing.

Figure 3 indicates the second harmonic maximum conversion efficiency variation as a function of ω_c/ω_0, for various values of the plasma density. The figure reveals that the harmonic radiation is completely different for strongly magnetized plasma, in comparison to the weakly magnetized case (jha *et al.*, 2007). The difference arises for dense and strongly magnetized plasma, when the effect of the polarization field dominates. It is clear from Figure 3 for sufficiently strong magnetic field, the second harmonic generation scenario is changed. For example, for $\omega_c/\omega_0 > 0.57$, the second harmonic generation is stopped for $\omega_p/\omega_0 = 0.6$ and drastically increased for $\omega_p/\omega_0 = 0.5$, however, based on the previous report (jha *et al.*, 2007) the second harmonic generation increased continuously by increasing ω_p/ω_0 for a given magnetic field. Furthermore, the figure predicts that the harmonic radiation cuts off, when the magnetic field strength increases up until the saturation strength B_{sat}. As the figure demonstrates, saturation strength decreases with density increasing.

In Figure 4, the maximum power efficiency variation plotted as a function of parameter ω_p/ω_0, for different values of magnetic field strength. The figure shows that for

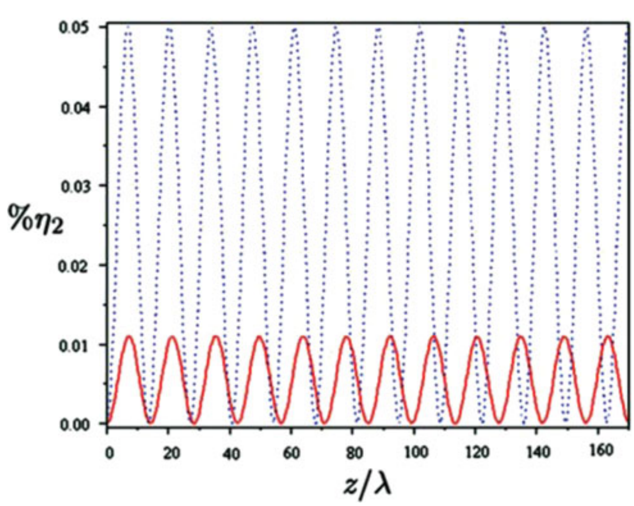

Fig. 2. (Color online) The phase-mismatch second harmonic conversion efficiency variation as a function of z/λ, for $\omega_p/\omega_0 = 0.3$, $a_1 = 0.271$. The solid line for $\omega_c/\omega_0 = 0.1$ and the point line for $\omega_c/\omega_0 = 0.2$.

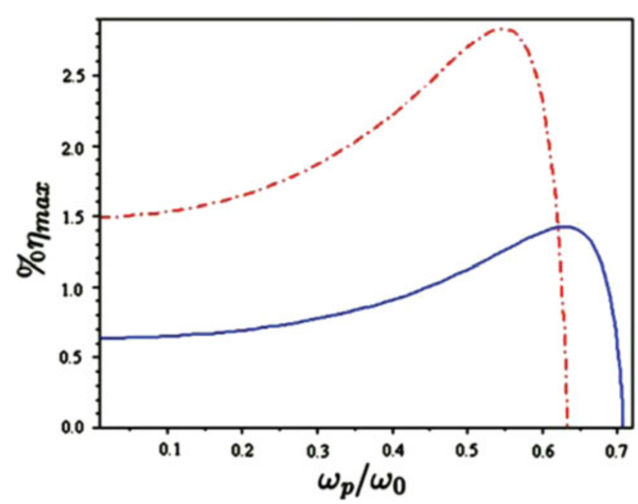

Fig. 4. (Color online) The maximum conversion efficiency variation for the phase-mismatch second harmonic with respect to the ω_p/ω_0, for $a_1 = 0.271$, respectively, the solid line for $\omega_c/\omega_0 = 0.5$, the dash dot line for $\omega_c/\omega_0 = 0.6$.

a constant magnetic field, the harmonic generation grows with density increasing. However, the harmonic radiation cuts-off, when the plasma density increases up until the saturation density n_{sat}. The saturation density depends on the applied magnetic field strength and increases for the weak magnetic field.

The conversion efficiency $\%\eta_3$ variation is plotted as a function z/λ, for the phase-mismatch third harmonic and for a non-magnetized plasma, in Figure 5. However, the power efficiency is very small, but it is important to note that the third harmonic can be generate for the non-magnetized case. In this figure, the dot line shows the average conversion efficiency, while the dash dot line indicates the conversion efficiency for the phase-match third harmonic (Esarey *et al.*, 1993; Gibbon, 1997; Mori *et al.*, 1993; Wilks *et al.*, 1993). Thus, the power efficiency slightly decreased for the phase-mismatch harmonic.

In Figure 6, we plot the maximum conversion efficiency variation for the third harmonic as a function of ω_c/ω_0, for various values of the plasma density. The figure shows that the harmonic radiation appreciably enhances by applying the external magnetic field. Like to the second harmonic, the third harmonic radiation stopped, when the magnetic field increased up to the saturation strength B_{sat}. The saturation strength increases for the low density plasma.

By tracking the values of the parameters ω_p/ω_0 and ω_c/ω_0, in one of the branches in Figures 3 and 6, anyone can find that the harmonics generation appreciably increase, when we get closest to the border line between $\epsilon_1 < 0$ and $\epsilon_1 > 0$, in Figure 1. For a point, which is exactly placed on the border line the harmonic generation stopped. Therefore, we can estimate the saturation magnetic field by making used of the condition $\epsilon_1 = 0$, as below:

$$B_{sat} = \frac{\omega_0 m}{e}\left(\frac{2\omega_p^2 - \omega_0^2}{\omega_p^2 - \omega_0^2}\right)^{1/2}, \tag{25}$$

where m and e, are the electron mass and charge, respectively.

Finally, the maximum conversion efficiency variation for the third harmonic is plotted as a function of ω_p/ω_0, for different values of magnetic field strength, in Figure 7. The figure shows that the harmonic radiation stopped, when the density increased up to the saturation density n_{sat}, while the applied magnetic field remains constant. The saturation

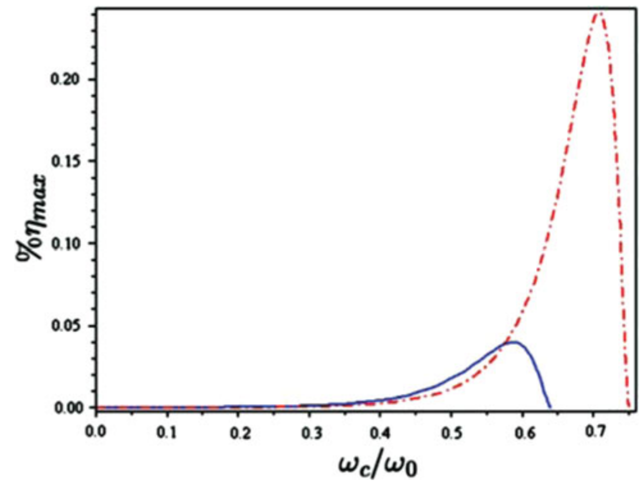

Fig. 6. (Color online) The maximum conversion efficiency variation for the the phase-mismatch third harmonic with respect to the ω_c/ω_0, for $a_1 = 0.271$, respectively, the solid line for $\omega_p/\omega_0 = 0.6$, the dash dot line for $\omega_p/\omega_0 = 0.5$.

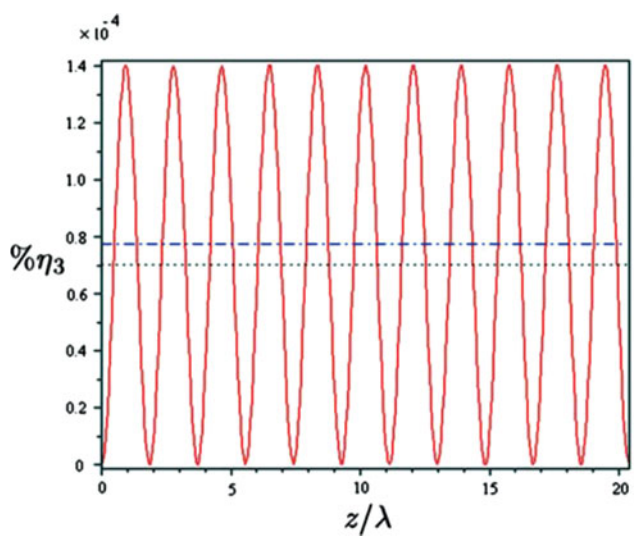

Fig. 5. (Color online) The phase-mismatch third harmonic conversion efficiency variation as a function of z/λ, for a non-magnetized plasma, $\omega_p/\omega_0 = 0.6$, $a_1 = 0.271$. The dot line shows the average phase-mismatch conversion efficiency and the dash dot line indicates the phase-matched conversion efficiency based on previous reports (Esarey *et al.*, 1993; Gibbon, 1997; Mori *et al.*, 1993; Wilks *et al.*, 1993).

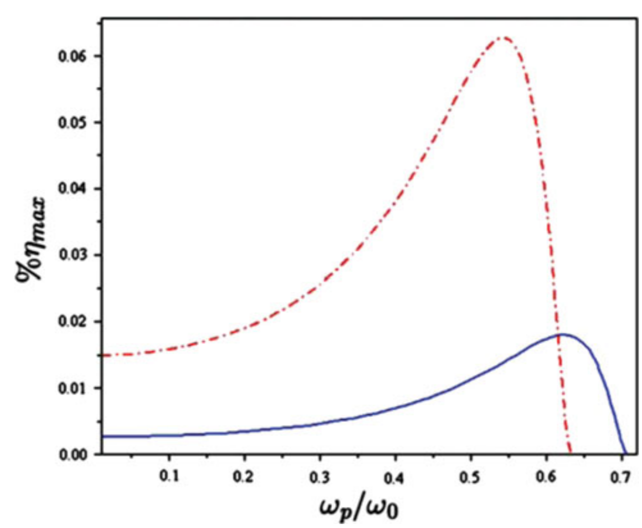

Fig. 7. (Color online) The maximum conversion efficiency variation for the phase-mismatch third harmonic with respect to the ω_p/ω_0, for $a_1 = 0.271$, respectively, the solid line for $\omega_c/\omega_0 = 0.5$, the dash dot line for $\omega_c/\omega_0 = 0.6$.

https://doi.org/10.1017/S0263034612000092 Published online by Cambridge University Press

density varies with magnetic field strength and decreases for the stronger magnetic field. The saturation density is accessible according to the condition $\epsilon_1 = 0$, as:

$$n_{sat} = n_{cr}\left(\frac{\omega_0^2 - \omega_c^2}{2\omega_0^2 - \omega_c^2}\right), \quad (26)$$

where $n_{cr} = m\epsilon_0\, \omega_0^2\, / e^2$ is the critical density.

4. SUMMARY AND CONCLUSION

In summary, we have investigated the conversion of a fraction of a laser beam to its second and third harmonics, in the interaction of intense laser field with transversely magnetized plasma. The plasma was dense and below the critical density, but the effect of the polarization field was considered. The harmonics radiation studied when there was a phase-mismatch between the phase velocities of the laser field and the generated harmonics. We proved the existence of a saturation magnetic field B_{sat}, in which the harmonics radiation stopped for $B \geq B_{sat}$. The strength of saturation field depended on the plasma density and increased for the low density plasma. This result arose owing to the polarization field effect in strongly magnetized dense plasma, and has not been reported previously. It is shown that for $B < B_{sat}$ the harmonics radiation appreciably enhanced with magnetic field increasing, however, the second harmonic disappeared in the absence of the magnetic field. We have investigated the existence of saturation density n_{sat}, where the harmonic radiation stopped for $n \geq n_{sat}$, while the applied magnetic field remained constant. In addition, we shown that for a non-magnetized plasma, the average phase-mismatch conversion efficiency was always a little below the phase-match one, for the third harmonic radiation. As a final, and important remark, it would be useful to note that, for sufficiently low density plasma we need a super strong magnetic field to get a maximum efficiency, so take into account that such strong field may be not accessible technically, we should be make a balance between the plasma density and the applied magnetic field to reach an optimum efficiency.

REFERENCES

Amendt, P., Eder, D.C. & Wilks, S.C. (1991). X-ray lasing by opticalfield-induced ionization. *Phys. Rev. Lett.* **66**, 2589.

Corkum, P.B. (1993). Plasma perspective on strong field multiphoton ionization. *Phys. Rev. Lett.* **71**, 1994.

Esarey, E., Ting, A., Sprangle, P., Umsladter, D. & Liu, X. (1993). Nonlinear analysis of relativistic harmonic generation by intense lasers in plasmas. *IEEE Trans. Plasma Sci.* **21**, 95.

Gibbon, P. (1997). High-order harmonic generation in plasmas. *IEEE Quant. Electron.* **33**, 1915.

Gorbunov, L.M., Mora, P. & Antonsen, T.M. (1997). Quasistatic magnetic field generated by a short laser pulse in an underdense plasma. *Phys. Plasmas* **4**, 4358.

Jha, P., Kumar, P., Upadhand, A.K. & Raj, G. (2005). Electric and magnetic wakefields in a plasma channel. *Phys. Rev. ST. Accel, Beam* **8**, 071301.

Jha, P., Mishra, R.K., Raj, G. & Upadhyay, A.K. (2007). Second harmonic generation in laser magnetized plasma interaction. *Phys. Plasmas* **14**, 053107.

Kienberger, R., Goulielmakis, E., Uiberacker, M., Baltuska, A., Yakovlev, V., Bammer, F., Scrinzi, A., Westerwalbesloh, Th., Kleineberg, U., Heinzmann, U., Drescher, M. & Krausz, F. (2004). Atomic transient recorder. *Nat.* **427**, 817.

Lemoff, B.E., Yin, G.Y., Gordan III., C.L., Barty, C.P.J. & Harris, S.E. (1995). Demonstration of a 10-Hz Femtosecond-Pulse-Driven XUV Laser at 41.8 nm in Xe IX. *Phys. Rev. Lett.* **74**, 1574.

Lin, H., Chen, L.M. & Kieffer, J.C. (2002). Harmonic generation of ultraintense laser pulses in underdense plasma. *Phys. Rev. E.* **65**, 036414.

Mori, W.B. (1993). Generation of coherent radiation using plasma. *IEEE Trans. Plasma Sci.* **21**, 1.

Mori, W.B., Decker, C.D. & Leemans, W.P. (1993). Relativistic harmonic content of nonlinear electromagnetic waves in underdense plasmas. *IEEE Trans. Plasma Sci.* **21**, 110.

Rax, J.M. & Fisch, N.J. (1992). Third-harmonic generation with ultrahigh-intensity laser pulses. *Phys. Rev. Lett.* **69**, 772.

Salieres, P. & Lewenstein, M. (2001). Generation of ultrashort coherent XUV pulses by harmonic conversion of intense laser pulses in gases: Towards attosecond pulses. *Meas. Sci. Technol.* **12**, 1818.

Sprangle, P., Esarey, E. & Ting, A. (1990). Nonlinear theory of intense laser -plasma interaction. *Phys. Rev. Lett.* **64**, 2011.

Tabak, M., Hammer, J., Glinsky, M.E., Kruer, W.L., Wilks, S.C. Woodworth, J., Campbell, E.M., Perry, M.D. & Mason, R.J. (1994). Ignition and high gain with ultrapowerful lasers. *Phys. Plasmas* **1**, 1626.

Tajima, T. & Dawson, J.M. (1979). Laser electron accelerator. *Phys. Rev. Lett.* **43**, 267.

Wilks, S.C., Kruer, W.L. & Mori, W.B. (1993). Odd harmonic generation of ultra-intense laser pulses reflected from an overdense plasma. *IEEE Trans. Plasma Sci.* **21**, 120.